Journal of Applied Polymer Science

Effect of Water-Absorbing Nanospheres on Antistatic Property of Isotactic Polypropylene Fibers

Hongxing Liu,[1] Jianguo Tang,[1] Yao Wang,[1] Linjun Huang,[1] Yanxin Wang,[1] Jiqing Jiao,[1] Jixian Liu,[1] Zhichao Xin,[1] Laurence A. Belfiore[1,2]

[1]Institute of Hybrid Materials, The National Base of International S. & T. Cooperation on Hybrid Materials and the Growing Base for State Key Laboratory, Qingdao University, 308 Ningxia Road, Qingdao 266071, People's Republic of China

[2]Department of Chemical and Biological Engineering, Colorado State University, Fort Collins, CO 80523

Correspondence to: J. Tang (E-mail: jianguotangde@hotmail.com) and L. A. Belfiore (E-mail: belfiore@engr.colostate.edu)

ABSTRACT: In this article, novel antistatic isotactic polypropylene (iPP) fibers were prepared through adding ternary polymer water-absorbing nanospheres (TPWANs) into iPP melt in melt spinning process. The TPWANs were synthesized through emulsion copolymerization of styrene (St), butyl acrylate (BA), and sodium allylsulfonate (SAS). The characterization results of Fourier transform infrared spectrometer (FT-IR) and ^{1}H nuclear magnetic resonance (^{1}H NMR) confirmed the ternary components in this copolymer. Transmission electron microscopy (TEM) images indicated the nanospherical shape of TPWANs with the characteristics of 80–90 nm size range of diameter and good dispersion in iPP fibers. The volume resistance of iPP fibers decreased by three orders from 10^{12} to 10^9 Ω cm when the 6 wt % TPWANs was added into iPP fibers, indicating that the blend fibers have good antistatic property. Most importantly, the nanospherical structure of TPWANs imparts both the compatibility and antistatic property into the blend iPP fibers.
 J. Appl. Polym. Sci. **2014**, *131*, 40568.

KEYWORDS: antistatic fibers; emulsion polymerization; nanospheres; sodium allylsulfonate; water-absorbing

Received 31 December 2013; accepted 8 February 2014

DOI: 10.1002/app.40568

INTRODUCTION

Isotactic polypropylene (iPP) fibers have widely been utilized in carpet, drapery, upholstery fabrics, and geotextiles for decades due to their good mechanical property, heat-resistant quality, low density, etc.[1,2] However, they are deficient in dispelling static charges in use because of intrinsic hydrophobicity of iPP. Thus, iPP fibers easily attract dusts, lead to electric shock, cause static powder explosion and generate serious damages in electronic industry.[3–5] To avoid these problems, the antistatic fibers must be developed by adding antistatic agents to polymer matrix during fabrication.[6]

There are publications on improving the antistatic property of iPP fibers.[7–9] We can classify them into four types: the first one is surface coatings or immersions of iPP fibers or fabrics with antistatic agent solutions, such as alkylphenol polyethylene ether, methyl silicone oil, PEG, or other hydrophilic compounds,[10] which provide simple and easy way but the durability of fibers are weak and easy to wash out. The second one is additions of amphiphilic additives in spinning process, such as alkane sulfonate, carboxylate, quaternary ammonium salt, etc. But the stability of iPP fibers to keep these compounds inside is weak and these additives are easy to migrate to fiber surface.[11] The third one is the additions of conductive fillers in spinning process, such as carbon blacks, carbon nanotubes, metallic fillers,[12–14] which can dispel the static charges intrinsically, but they introduce some problems into fiber products. For example, carbon blacks or carbon nanotubes[12] offer the black color, and metal powders provide worse mechanical property due to high filling. In some cases, the cost of fiber production also increases.[13] The forth one is the blends with polymer antistatic agents in fibers, in which the water absorbing components can be introduced by copolymers containing polar monomers[15] through melt blending spinning process. By this strategy, the compatibility of antistatic agents with iPP matrix becomes a key factor. In melt spinning process, the additives develop into nebulization from blending melt and separate from forming fibers. Comparing the four ways to improve the antistatic property of iPP fibers, the forth one has its polymer–polymer blend advantage, but the compatibility and water absorbing capability for a polymeric additives are conflict factors.

To have both compatibility and water absorbing capability in a single polymeric antistatic additive, recent investigations try to get the compromise between them. Xu et al.[1] reported that

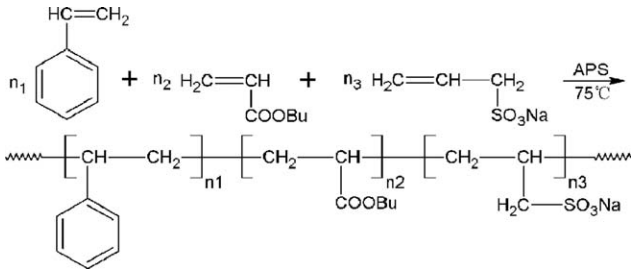

Scheme 1. Illustration of the synthesis reaction of ternary polymer water-absorbing nanospheres (TPWANs) by emulsion polymerization.

polyethylene wax grafted with sodium acrylate (PEW-g-AAS) and polypropylene grafted with sodium acrylate (PPW-g-AAS). They found that PPW-g-AAS has an inferior antistatic performance although it has better compatibility, while PEW-g-AAS is contrast to it. Wang et al.[16] fabricated hybrid additive of poly (sodium acrylate) modified multiwalled carbon nanotubes and silver nanoparticles for antistatic polyetherimide (PEI). However, the polar property of poly (sodium acrylate) as covering agent makes worse compatibility of this antistatic additive. On the other hand, the endeavor to use quaternary ammonium salt ion-conductive (QASI) compound as antistatic agent also confirmed the compatibility problems.[17]

In this work, ternary polymer water-absorbing nanospheres (TPWANs) served as antistatic agent was prepared by emulsion polymerization of styrene (St), butylacrylate (BA), and sodium allylsulfonate (SAS). Antistatic iPP fibers prepared by melt spinning with this antistatic agent confirm the available compromise between compatibility and water absorbing capability. The resulted fibers have excellent antistatic properties.

EXPERIMENTAL

Materials

St (AR) was purchased from Yongda Chemical Company, purified by a basic alumina column to remove the inhibitors. BA (AR) was provided by Guangfu Fine Chemical Research Institute, purified by washing of a 5 wt % NaOH aqueous solution for three times to remove inhibitions, and then washed with deionized water for it to be neutral. SAS (98%, AR), ammonium per sulfate (APS, AR) and sodium dodecyl sulfate (SDS, AR) were purchased from Guang Cheng Chemical Company without further purification. iPP was provided by Sinopec Qingdao Refining and Chemical Company. The other reagents used in this experiment were analytical grade.

Synthesis of Water-Absorbing Nanospheres

The synthesis of water-absorbing nanospheres was referred to the literature.[18,19] Water-absorbing nanospheres were prepared by a semicontinuous emulsion polymerization as shown in Scheme 1. 2 g SDS, 2 g SAS, and 25 g deionized water were added into a 250 mL three-neck round flask equipped with a reflux condenser and a nitrogen inlet. The mixture was stirred with a magnetic bar at 300 rpm to homogenize at room temperature. After about 10 min, the mixture of St (18 g) and BA (22 g) were added into the flask for pre-emulsification at room temperature for 30 min. Then, a half of pre-emulsification solution was taken out from the flask, and then 50 g deionized water was added into the flask. Subsequently, the remaining solution was heated to 75°C under nitrogen purging. 0.1 g of APS was introduced by dropwise addition under stirring. The reaction continued until there is no refluxing of monomers. And then, another half of pre-emulsification solution and 0.1 g of APS were introduced by dropwise addition into the system within 3 h. After an additional 1 h reaction at 75°C, the final TPWANs were obtained when finishing the filtration of the product in the flask.

Preparation of Antistatic iPP Fibers

Preparation of Master Batch. iPP chips (336 g) and TPWANs (84 g) were blended for 5 min, and then extruded at 210–220°C in a mini Twin Screw Compounder (DSM Xplore, The Netherlands).

Melt Spinning of iPP with Master Batch. iPP chips and a certain amount of the master batch (1–6 wt %) mentioned above were mingled, and then dried in a vacuum oven at 100°C under 0.01 MPa for 6 h. The melt spinning was carried at 220°C on a spinning machine (Linzi Fangchen Co.). The spun filaments were air-cooled, and wound up at 445 m min^{-1}.

Characterization. The Fourier transform infrared spectrometer (FT-IR), Nicolet 5700, was used to measure the components of the prepared TPWANs and iPP fibers in the wavenumber range of from 400 to 4000 cm^{-1}.

NMR measurement was carried on a ^1H nuclear magnetic resonance (^1H NMR) spectroscope, [JNM-ECP600 (600 MHz), JEOL, Japan] with $CDCl_3$ as the solvent and tetramethylsilane (TMS) as the internal standard.

X-ray diffraction (XRD) measurement was carried out on a D-8 Advance X-ray diffractometer. The scan rate is 5°min^{-1} in the 2θ range of 10°–70°.

The particle size and size distribution of TPWANs were investigated by a laser scattering instrument, a particle size analyzer (MICROTRAC, INC. SERIAL NO. U2515). Before measurement, the emulsion taken from reaction flask was diluted to 0.1 wt % solid content with deionized water. The results of particle size were obtained by calculating the average values of three measurements.

Transmission electron microscope (TEM) used in this work was a JEM-1200EX, by which we observed the morphological structures of both original TPWANs and the blend iPP fibers. The polymerized raw emulsion was diluted with deionized water, dropped on to a copper grid and stained with phosphotungstic acid. For observations of iPP blend fibers, the fibers were embedded by epoxy resin before cut into ultrathin slices. After stained by RuO_4,[20] the ultrathin slices were used to observe.

Differential scanning calorimeter (DSC, TA Instruments Q20) was used to study the crystallization behavior of iPP fibers. The scanning temperature ranges within 0–250°C with the heating rate at 10°C min^{-1} under nitrogen purging.

The volume resistance of blend iPP fibers was tested on a LCK-306 resistance meter (Shandong textile research institute, China) in standard environmental conditions of 65% relative humidity and 25°C temperature.

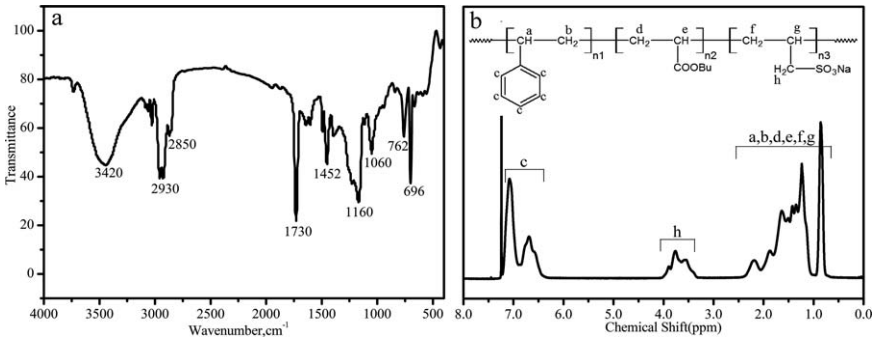

Figure 1. FT-IR spectrum of TPWANs (a) and ^{1}H NMR spectrum of TPWANs (b).

The weighing method was used to determine the loss weight ratio (LWR) according to eq. (1) below:

$$\mathrm{LWR} = \frac{W_0 - W_1}{W_0} \times 100\% \quad (1)$$

where W_0 and W_1 are the weights of fibers before and after washing, respectively. Here, the used fibers were washed in boiling water at 100°C for 1 h, and then dried to constant weight.

Similarly, the water uptake ratio (WUR) was determined by eq. (2) below:

$$\mathrm{WUR} = \frac{W_1 - W_2}{W_2} \times 100\% \quad (2)$$

where W_1 and W_2 are the weights of wet and dry fibers, respectively. The used fibers were dried to constant weight in an oven at 100°C, and then placed in room temperature for 1 day.

RESULTS AND DISCUSSION

Characterization of Morphological Structures and Size Distribution of TPWANs

FT-IR measurement results were shown in Figure 1(a). The characteristic absorption bands at 696 and 762 cm^{-1} correspond to benzyl groups. The characteristic absorption bands at 1060 and 1160 cm^{-1} are attributed to the stretching vibrations of S═O double bond in SAS. The band at 1730 cm^{-1} is caused by the stretching vibration absorption of carbonyl (C═O) double bond in BA. Thus, those results confirm that TPWANs are the ternary copolymer containing St, BA, and SAS. At the same time, TPWANs were characterized by ^{1}H NMR, shown in Figure 1(b). The peaks at 0.84–2.14 ppm are correspond to H chemical shift for a, b, d, e, f, g in this copolymer. The peaks at 3.58–3.77 ppm are correspond to H chemical shifts for h that is close to —SO_3Na in SAS. The chemical shift of H atom in —C_6H_5 group appear in the range of 6.68–7.11 ppm that correspond to the benzyl conjugate influence. Thus, ^{1}H NMR spectrum proves the TPWAN components too.

The XRD pattern of TPWANs at room temperature was shown in Figure 2. One can find the typical amorphous diffraction peak around $2\theta = 20°$. There is no noticeable crystal diffraction characteristic in the random copolymer of TPWANs.[21]

Figure 3 shows TEM image and particle size measurement result. The shape of TPWANs is almost round spheres with fairly smooth surface. The TPWAN diameters almost are roughly in the range of 80–90 nm. On the other hand, the size analyzer indicates that the most probable size is 87 nm with a narrow distribution. Obviously, the results from TEM and size analyzer highly coincide to confirm the particle size of TPWANs.

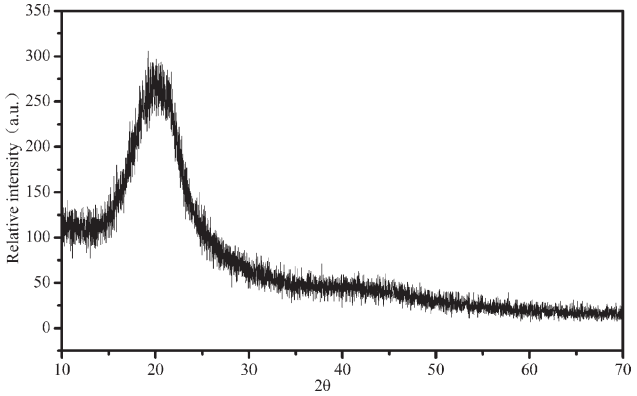

Figure 2. X-ray diffraction pattern of TPWANs.

Composition and Morphological Structure of Antistatic iPP Fibers

Figure 4 shows FT-IR spectra of iPP fibers with different contents of TPWANs from 0 to 6%. The absorption bands at 2954, 2844, 1456, 1375, 1163, and 977 cm^{-1} belong to the

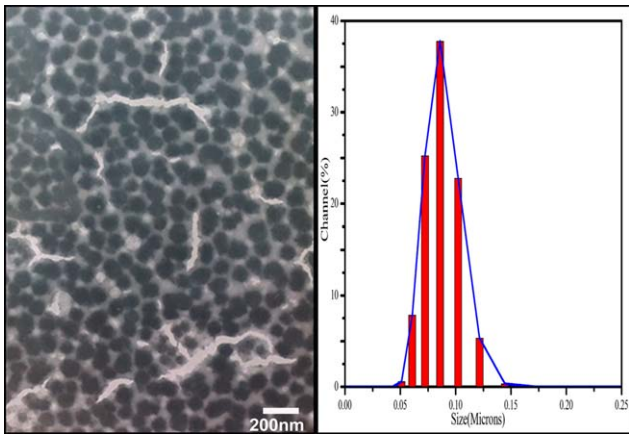

Figure 3. TEM image and size analyzing results of TPWANs. [Color figure can be viewed in the online issue, which is available at wileyonlinelibrary.com.]

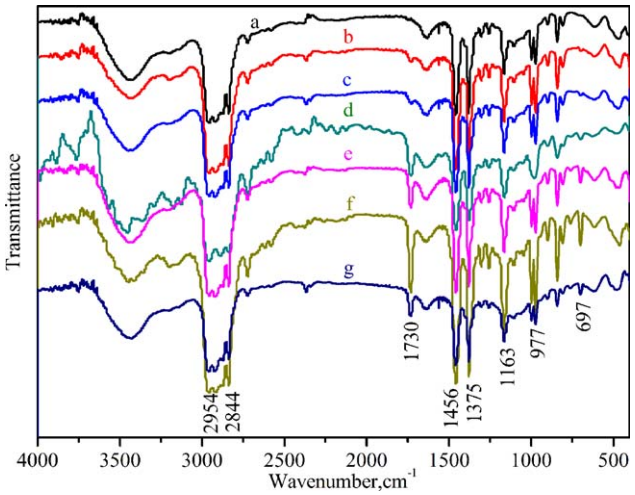

Figure 4. FT-IR spectra of iPP fibers with different content of TPWANs (contents of TPWANs in iPP fibers from a to g were 0–6 wt %, respectively). [Color figure can be viewed in the online issue, which is available at wileyonlinelibrary.com.]

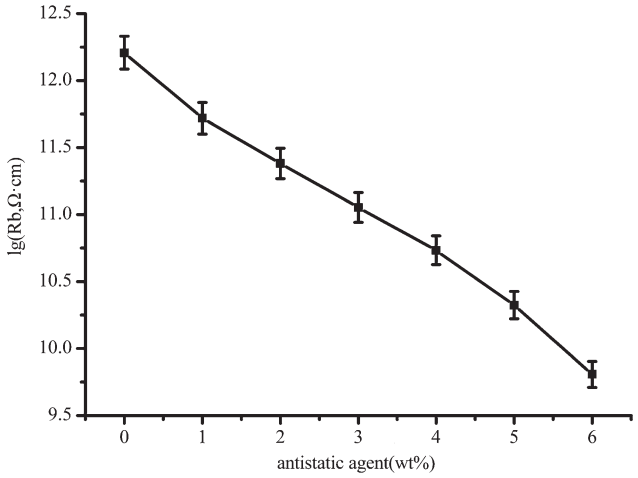

Figure 6. Volume resistance of iPP fiber with different content of TPWANs.

characteristic vibrations of iPP in all spectra. Whereas, in the spectra of TPWANs contents from 1 to 6%, we can find the characteristic absorption bands of carbonyl group (C═O) at 1730 cm^{-1} and of benzyl group at 697 cm^{-1}, respectively. The intensities corresponding to the both groups increase with the increases of TPWAN contents in iPP fibers. Thus, we can confirm the existence of TPWANs in iPP fibers.

The distribution of TPWANs in iPP fibers was evaluated by TEM (Figure 5). Based on the seven images from a to g in

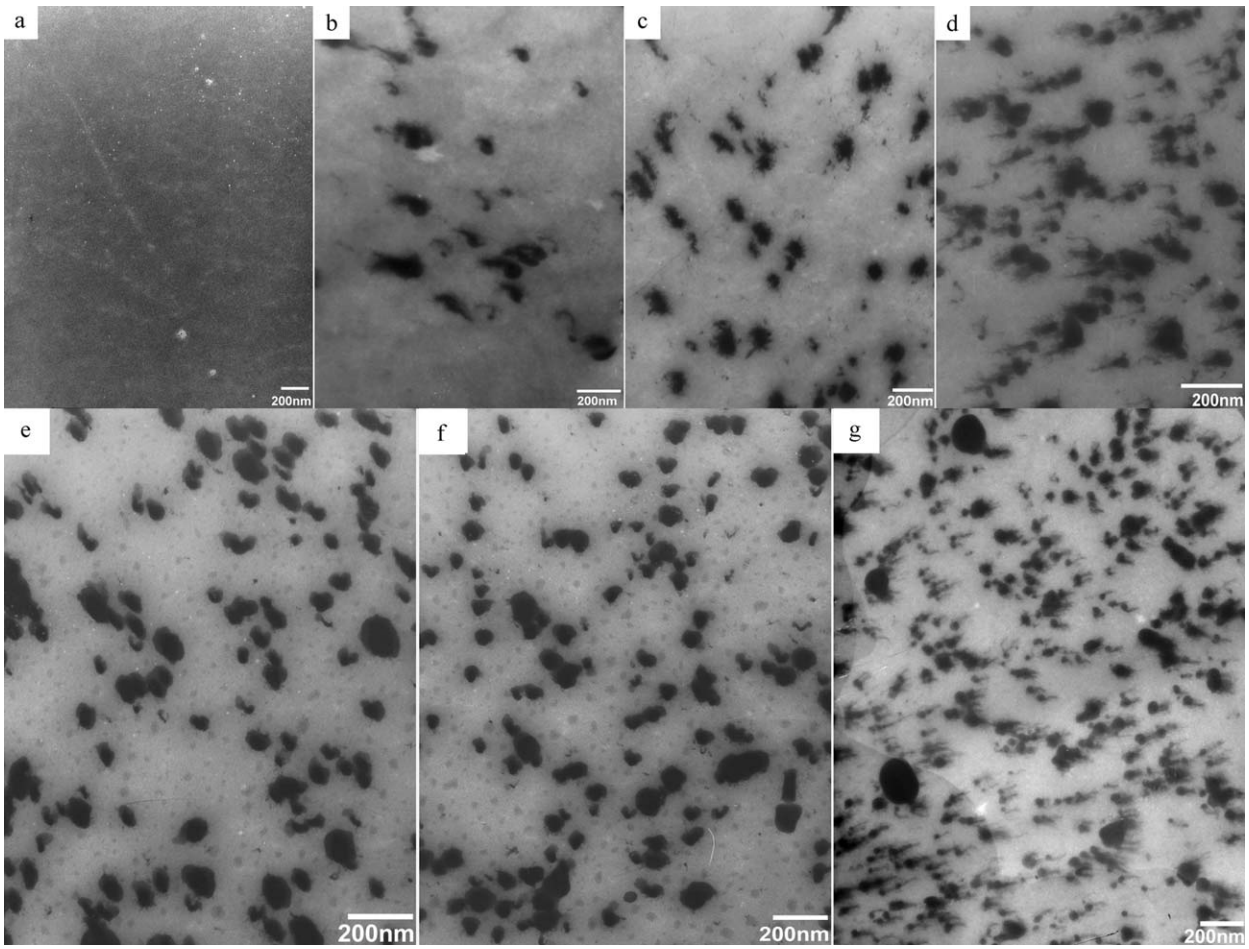

Figure 5. TEM images of antistatic iPP fibers (contents of TPWANs in iPP fibers from a to g were 0–6 wt %, respectively).

Table I. The Water Uptake Ratios of iPP Fibers[a]

Sample	0	1	2	3	4	5	6
WUR (%)	0.33	0.39	0.42	0.45	0.47	0.51	0.56

[a] Contents of TPWANs in iPP fibers from samples 0 to 6 is 0–6 wt %, respectively.

Table II. The Loss Weight Ratio of iPP Fibers[a]

Sample	0	1	2	3	4	5	6
LWR (%)	0.012	0.014	0.017	0.021	0.026	0.031	0.033

[a] Contents of TPWANs in iPP fibers from samples 0 to 6 is 0–6 wt %, respectively.

Figure 5, the good dispersion of TPWANs in the iPP fiber matrix is clearly shown. However, the geometrical parameters have obvious changes. The shape becomes noncircular and the size distribution becomes wider. Only a few of TPWANs keep their diameter at about 87 nm, and most of them reduce its size into 40–70 nm. The smaller size and noncircular shape are obviously caused by shear deformation in melt spinning process, and indicate a very important fact that TPWANs were deformed and slightly broken.

Antistatic Effects of TPWANs in iPP Fibers

The decrease of the volume resistance of iPP fibers is considered as the measurement of antistatic property of TPWANs as antistatic agent. Figure 6 indicates that virgin iPP fiber without TPWANs has the highest volume resistance, 10^{12} Ω cm, while remarkable decrease of volume resistance were observed with the increase of added TPWANs in iPP fibers from 1 to 6 wt %. The lowest volume resistance, 10^{9} Ω cm, is indicated when the content of TPWANs reached to 6 wt %. Following the consideration that the taking-up water in fibers will improve the antistatic property,[22,23] we evaluated the water uptake values of blend iPP fibers containing TPWANs from 0 to 6 wt % and the results listed in Table I, which indicates that the water uptake ratio (WUR) increases from 0.33 to 0.56% with the increase of added TPWANs. These results coincide the principle of absorbed-water dispelling static charges.

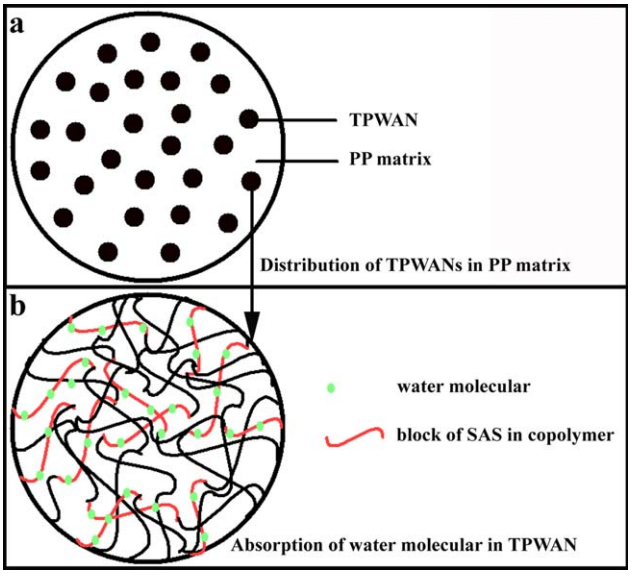

Figure 7. Mechanism of the absorption of moisture. [Color figure can be viewed in the online issue, which is available at wileyonlinelibrary.com.]

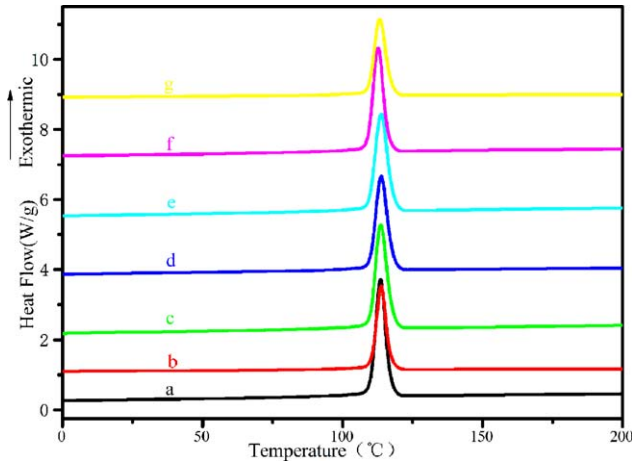

Figure 8. DSC results of iPP fiber with different content of TPWANs (contents of TPWANs in iPP fibers from a to g were 0–6 wt %, respectively). [Color figure can be viewed in the online issue, which is available at wileyonlinelibrary.com.]

Different from the previous direct blend of iPP with polar polymers, the TPWANs in this work have good *in situ* keeping stability in iPP fibers. Previous publications[24,25] for blend fibers with antistatic polymer additives concern about the loss weight when they were cooked in boiling water for an expected time period. Table II shows the loss weight ratios (LWR) of blended iPP fibers in this work. The LWR values just have slight increase when the added TPWANs reach to 6 wt %. The total loss weight still is at very low level. Compare with references value of 0.15–0.42% for antistatic fibers,[24] this indicates that TPWANs have a good compatibility with iPP matrix in this work.

Actually, the stability and the antistatic property root in the special structure of TPWANs. Figure 7(a) diagrammatically indicates the morphology of TPWANs in iPP fibers, in which TPWANs are small islands. Figure 7(b) shows the mechanism of water absorption of TPWANs. In the small nanospheres, hydrophilic units of SAS in ternary polymer richly take up water molecules that fulfill the entire nanosphere. Thus, we can think that the dispersed TPWANs in iPP fibers like small "nano-reservoirs" that store water for fibers. On the other hand, these "nano-reservoirs" include hydrophobic components in ternary polymers that provide the compatibility with iPP matrix. Most importantly, the essential difference of TPWANs from other amphiphilic polymeric additives is that TPWANs concentrates the hydrophilic units within nanospheres while other two hydrophobic components can behave their compatibility with iPP at the nanospheric surface. Hence, the iPP fibers have the superior antistatic ability at the content of 6 wt % TPWANs.

Crystallization Behavior of iPP Fibers

iPP is a crystalline polymer. There are compounds, inorganic nanoparticles and polymers can behave the nucleating effect on it.[9,26–31] Figure 8 shows DSC measurement results of iPP fibers including TPWANs, from which we can not find the obvious differences of crystallization temperature and crystallization peak areas. This means that there is no nucleating effect of TPWANs on iPP crystallization.

CONCLUSIONS

In this work, TPWANs were synthesized. They play as a good antistatic agent for iPP fibers. The results show that the synthesized TPWANs can effectively improve the antistatic ability of iPP fibers when they added into the melt of iPP in melting process. TPWANs can disperse evenly in iPP matrix. The assembly of hydrophobic and hydrophilic in the same nanospheres provides the good compromise of compatibility and stability of TPWANs in iPP matrix.

ACKNOWLEDGMENTS

The authors appreciate the financial supports from: (1) The National One-Thousand Foreign Expert Program (WQ20123700111); (2) Natural Scientific Foundation of China, Grant #51273096; (3) Natural Scientific Foundation of China, Grant #51373081; (4) Shandong Province Project: Tackle Key Problem in Key Technology, #2010GGX10327; (5) Program of Qingdao Science and Technology, #12-1-4-2-(8)-jch.

REFERENCES

1. Xu, X.; Xiao, H.; Guan, Y.; Li, S.; Wei, D.; Zheng, A. *J. Appl. Polym. Sci.* **2012**, *126*, 83.
2. Bajaj, P.; Gupta, A.; Ojha, N. *J. Macromol. Sci, Part C: Polym. Rev.* **2000**, *40*, 105.
3. Dudler, V.; Grob, M. C.; Mérian, D. *Polym. Degrad. Stab.* **2000**, *68*, 373.
4. Kobayashi, T.; Wood, B. A.; Takemura, A.; Ono, H. *J. Electrostat.* **2006**, *64*, 377.
5. Maki, N.; Nakano, S.; Sasaki, H. *Packag. Technol. Sci.* **2004**, *17*, 249.
6. Lehmann, W. *Kunst. Ger. Plast.* **1992**, *82*, 991.
7. Brown, D.; Pailthorpe, M. M. *Rev. Color. Technol.* **1986**, *16*, 8.
8. Holme, I. *Int. J. Adhes. Adhes.* **1999**, *19*, 455.
9. Seo, M.-K.; Lee, J.-R.; Park, S.-J. *Mat. Sci. Eng: A Struct.* **2005**, *404*, 79.
10. Xu, D.; Guo, J.; Liang, T. *Fangzhi Xue Bao* **1997**, *18*, 16.
11. James, W.; Simmons, R.; Chatham, P. *Plast. Build. Construct.* **1999**, *23*, 10.
12. Li, C.; Liang, T.; Lu, W.; Tang, C.; Hu, X.; Cao, M.; Liang, J. *Compos. Sci. Technol.* **2004**, *64*, 2089.
13. Cai, Y.; Ma, S. *Adv. Mater. Res.* **2013**, *821–822*, 99.
14. Kumar, S.; Doshi, H.; Srinivasarao, M.; Park, J. O.; Schiraldi, D. A. *Polymer* **2002**, *43*, 1701.
15. Yamato, Y.; Watanabe, Y. U.S. Patent 8, 183, 324, May 22, **2012**.
16. Wang, Y.; Zhang, C.; Du, Z.; Li, H.; Zou, W. *Synth. Met.* **2013**, *182*, 49.
17. Bao, L.; Lei, J.; Wang, J. *J. Electrostat.* **2013**, *71*, 987.
18. Tang, J.; Yang, B.; Liu, J.; Wang, Y.; Huang, L.; Huang, Z.; Wang, Y.; Zhu, Q.; Belfiore, L. A. *RSC Adv.* **2012**, *2*, 8813.
19. Yang, B.; Tang, J.; Yang, P.; Wang, Y.; Liu, J.; Liu, H.; Wang, R.; Huang, Z.; Liu, J.; Belfiore, L. A. *J. Appl. Polym. Sci.* **2012**, *126*, 706.
20. Trent, J. S.; Scheinbeim, J. I.; Couchman, P. R. *Macromolecules* **1983**, *16*, 589.
21. Ha, J.-W.; Park, I. J.; Lee, S.-B.; Kim, D.-K. *Macromolecules* **2002**, *35*, 6811.
22. Li, K.; Zhang, C.; Du, Z.; Li, H.; Zou, W. *Synth. Met.* **2012**, *162*, 2010.
23. Lou, L. *Adv. Mater. Res.* **2012**, *167*, 573.
24. Jin, Y.; Gao, X.; Liu, G. *Polym. Mater. Sci. Eng.* **2001**, *17*, 153.
25. Jin, Y. The study of a new kind of antistatic PET fiber. Dissertation for Doctoral Degree at Sichuan University, **2008**.
26. Bhattacharyya, A. R.; Sreekumar, T. V.; Liu, T.; Kumar, S.; Ericson, L. M.; Hauge, R. H.; Smalley, R. E. *Polymer* **2003**, *44*, 2373.
27. Lee, G.-W.; Jagannathan, S.; Chae, H. G.; Minus, M. L.; Kumar, S. *Polymer* **2008**, *49*, 1831.
28. Zhang, Y.; Wu, H.; Qiu, Y. *Bioresour. Technol.* **2010**, *101*, 7944.
29. Wang, M.; Lin, L.; Peng, Q.; Ou, W.; Li, H. *J. Appl. Polym. Sci.* **2013**, *131*, doi:10.1002/app.39632.
30. Wang, S.; Zhang, J. *Sol. Energ. Mat. Sol. C* **2013**, *117*, 577.
31. Diez-Pascual, A. M.; Naffakh, M. *ACS Appl. Mater. Inter.* **2013**, *5*, 9691.